NREL
NATIONAL RENEWABLE ENERGY LABORATORY

Passive Two-Phase Cooling of Automotive Power Electronics

Preprint

G. Moreno, J. R. Jeffers, S. Narumanchi, and K. Bennion

Presented at SEMI-THERM 2014
San Jose, California
March 9–13, 2014

NREL is a national laboratory of the U.S. Department of Energy
Office of Energy Efficiency & Renewable Energy
Operated by the Alliance for Sustainable Energy, LLC

This report is available at no cost from the National Renewable Energy Laboratory (NREL) at www.nrel.gov/publications.

Conference Paper
NREL/CP-5400-61083
August 2014

Contract No. DE-AC36-08GO28308

NOTICE

This report is available at no cost from the National Renewable Energy Laboratory (NREL) at www.nrel.gov/publications.

Available electronically at http://www.osti.gov/scitech

Available for a processing fee to U.S. Department of Energy and its contractors, in paper, from:

U.S. Department of Energy
Office of Scientific and Technical Information
P.O. Box 62
Oak Ridge, TN 37831-0062
phone: 865.576.8401
fax: 865.576.5728
email: mailto:reports@adonis.osti.gov

Available for sale to the public, in paper, from:

U.S. Department of Commerce
National Technical Information Service
5285 Port Royal Road
Springfield, VA 22161
phone: 800.553.6847
fax: 703.605.6900
email: orders@ntis.fedworld.gov
online ordering: http://www.ntis.gov/help/ordermethods.aspx

Cover Photos: (left to right) photo by Pat Corkery, NREL 16416, photo from SunEdison, NREL 17423, photo by Pat Corkery, NREL 16560, photo by Dennis Schroeder, NREL 17613, photo by Dean Armstrong, NREL 17436, photo by Pat Corkery, NREL 17721.

Passive Two-Phase Cooling of Automotive Power Electronics

Gilberto Moreno*, Jana R. Jeffers, Sreekant Narumanchi, and Kevin Bennion
National Renewable Energy Laboratory
Golden, CO, USA
*gilbert.moreno@nrel.gov

Abstract

Experiments were conducted to evaluate the use of a passive two-phase cooling strategy as a means of cooling automotive power electronics. The proposed cooling approach utilizes an indirect cooling configuration to alleviate some reliability concerns and to allow the use of conventional power modules. An inverter-scale proof-of-concept cooling system was fabricated and tested using the refrigerants hydrofluoroolefin HFO-1234yf and hydrofluorocarbon HFC-245fa. Results demonstrated that the system can dissipate at least 3.5 kW of heat with 250 cm^3 of HFC-245fa. An advanced evaporator concept that incorporates features to improve performance and reduce its size was designed. Simulation results indicate the concept's thermal resistance can be 58% to 65% lower than automotive dual-side-cooled power modules. Tests were also conducted to measure the thermal performance of two air-cooled condensers—plain and rifled finned tube designs. The results combined with some analysis were then used to estimate the required condenser size per operating conditions and maximum allowable system (i.e., vapor and liquid) temperatures.

Keywords

Power electronics, thermal management, two-phase heat transfer

Nomenclature

A	area, cm^2
P	pressure, MPa
R''_{th}	unit/area-weighted thermal resistance, cm^2-K/W
T	temperature, °C

Subscripts:

a	air
c	critical (e.g., critical pressure)
htr	heater
j	junction
l	liquid
r	reference (e.g., reference area)
sat	saturated
v	vapor

1 Introduction

Improved thermal management is an enabling strategy to increase power densities, increase reliability, and reduce cost of electronic devices. Traditionally, single-phase liquid cooling strategies have been employed to cool power electronics in electric-drive vehicles. Improvements to the automotive power module's thermal resistance, for the most part, have been focused on reductions to the passive stack thermal resistance. Significant improvements in power electronics thermal management can also be achieved using more aggressive cooling techniques (i.e., two-phase heat transfer). The high heat transfer rates of two-phase heat transfer allow for increased power density and specific power that may enable achieving the U.S. Department of Energy's Advanced Power Electronics and Electrical Motors Program technical targets.

1.1 Conventional Automotive Power Electronics Cooling Strategies

Liquid cooling solutions are commonly used for cooling power electronic devices. Water-ethylene glycol (WEG)-based cooling strategies are well understood in terms of performance and reliability and thus are widely used in automotive power electronics cooling applications. Liang [1] has experimentally characterized junction-to-liquid thermal resistances for the 2010 Nissan Leaf and 2010 Toyota Prius power modules. One of the more effective WEG-based cooling strategies is a dual-side-cooling approach implemented in the 2008 Lexus Hybrid [2, 3]. The dual-side cooling approach of this system allows for greater heat dissipation per die footprint as compared to the more traditional single-side cooled modules that are more typical of automotive applications.

1.2 Two-Phase Based Cooling Alternatives

Two-phase-based cooling strategies have been studied in as a means of increasing device power densities. Ayers et al. [4] proposed a two-phase-based cooling strategy where the power electronics cooling system can be combined with the automotive air-conditioning system. In their approach, the power electronics were immersed in HFC-134a resulting in a reported 50% inverter volume reduction. Barnes and Tuma [5] evaluated passive and immersion two-phase cooling of power electronics. Heat fluxes in excess of 1,000 W/cm^2 were reported using a passive two-phase cooling approach. Based on their tests, it was estimated that refrigerant requirements for a passive immersion cooling system could be on the order of 100 cm^3 of refrigerant per kilowatt of heat dissipated. In addition, an in-situ degassing technique to remove air that may infiltrate the system was described. Performance characteristics of various air-cooled condenser designs operating in thermosyphon configurations and charged with hydrofluoroether fluids are reported by Tuma et al. [6].

Various two-phase-based thermosyphon cooling concepts have been explored for a variety of electronics cooling applications. Franco and Filippeschi [7] published a literature review of thermosyphons dissipating less than 1 kW of heat. They discuss differences in experimental design and attempt

to explain the lack of generalized results for all data sources reviewed. Difficulty in comparing data arises due to differences in physical design and possible presence of non-condensable gases in the system. Khodabandeh [8] explored the effects of fluid properties, system pressure, heat flux, mass flow rate, vapor friction, diameter of evaporator channel, and tubing distance between the evaporator and condenser on thermosyphon performance. Isobutane was used as the working fluid for all experiments. Of all the parameters tested, heat flux and reduced pressure were the most influential. Results indicated that nucleate boiling was the dominant mode of heat transfer in the evaporator. Similarly, Ramaswamy et al. [9] investigated the combined effects of sub-cooling and system pressure on thermosyphons with fluorocarbon FC-72 as the working fluid. It was determined that the combined effect of pressure and sub-cooling was to lower wall superheat.

Agostini et al. [10] designed a small thermosyphon for use in electronics cooling. A mathematical model was used to design the condenser, and the modeling results were compared against experimental results. The system consisted of an evaporator mounted to the power electronics, a vapor riser, an air-cooled condenser, and a liquid downcomer. In their study critical heat flux was not reached but heat rejection of up to 1.5 kW was reported. Khrustalev [11] evaluated the performance of two evaporators used in parallel (two separate evaporators connected via manifold to the same condenser) in an electronics cooling thermosyphon application. Methanol and ethyl alcohol were chosen as working fluids. It was reported that a loop thermosyphon is advantageous over a traditional heat pipe for electronics cooling. In a similar application, Pal et al. [12] used a small thermosyphon to cool a computer microprocessor with water and performance fluid PF5060. The evaporator and condenser were separated by a rising vapor tube and a liquid downcomer tube. Water was observed to outperform the dielectric liquid, providing a thermal resistance about 40% that of PF5060. In addition to studying the thermal performance of the two liquids, Pal et al. [12] studied the effects of inclination and found that evaporator surface temperatures remain uniform for inclination angles from -58° to +36°.

In this study, we evaluate a passive two-phase strategy as a means of improving thermal management of automotive power electronics. The intent is to utilize the high heat transfer rates associated with phase-change heat transfer to increase device power densities. A proof-of-concept cooling system, designed to cool six power modules, was fabricated. Experiments were conducted with refrigerants HFO-1234yf and HFC-245fa to determine if the system could dissipate the expected automotive heat load. Simulations were then performed to estimate the performance of an advanced evaporator design. The simulation thermal performance results were then compared with the performance of conventional automotive WEG based cooling systems. Condenser experimental results and analysis lead to condenser sizing requirements based on operating conditions and a maximum allowable system temperature.

2 Experimental Apparatus and Procedures

A proof-of-concept passive two-phase cooling system was designed and fabricated. Figure 1 shows the schematic of the cooling system that consists of an evaporator and an air-cooled condenser. The design cools automotive power modules consisting of six Delphi discrete power modules/switches. The six power modules represent a voltage source inverter system required to power an automotive electric machine/motor.

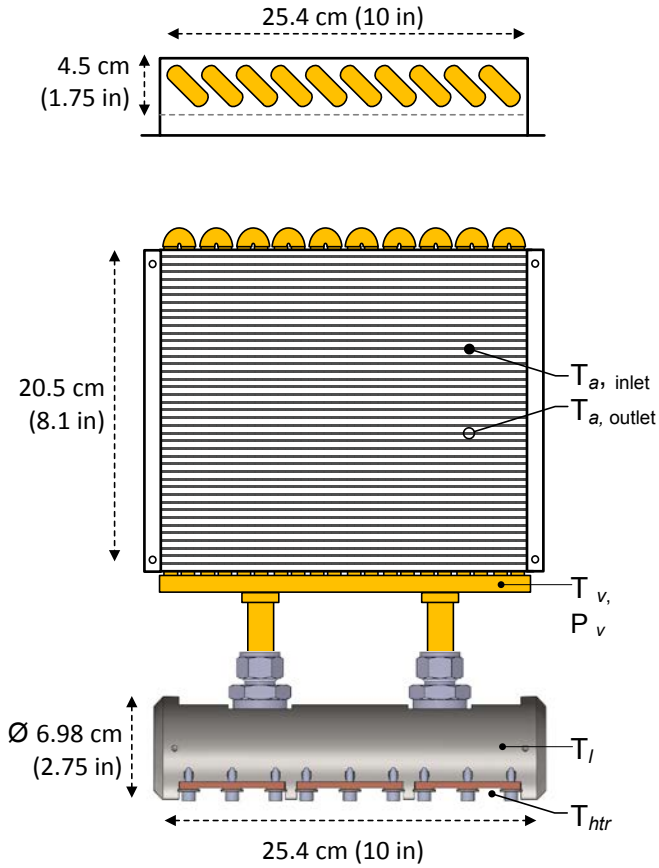

Figure 1: Schematic of the passive two-phase cooling system.

The system was designed with a maximum operating pressure of 1.03 MPa (150 psi). Structural finite element analyses (FEA) were used to design the system components for the elevated pressure requirements. Once fabricated, the system was hydrostatically pressure-tested to verify the system's pressure rating. The system's pressure rating provided flexibility by allowing it to be charged with refrigerant HFO-1234yf or HFC-245fa. System vapor pressure was measured using an absolute pressure transducer. System temperatures were measured using calibrated K-type thermocouples for the inlet-air, outlet-air, liquid, vapor, and heater temperatures.

A cross-sectional view of the evaporator is provided in Figure 2. The evaporator consists of a stainless steel cylinder and three copper cold plates. For this proof-of-concept system, steel was used instead of aluminum because it is easier to weld leak-free joints with steel. As will be discussed

later, future designs will incorporate brazed aluminum evaporators. The copper cold plates were machined with 4-mm-tall fins, each of which has a wetted surface area of about 55 cm^2. Because two-phase cooling provides high heat transfer rates, the fins are not expected to have a significant effect on the evaporator thermal resistance. However, the fins were included as a means of increasing surface area in an attempt to delay dry-out. No surface enhancement coatings were applied to the cold plates, leaving the finned surfaces smooth.

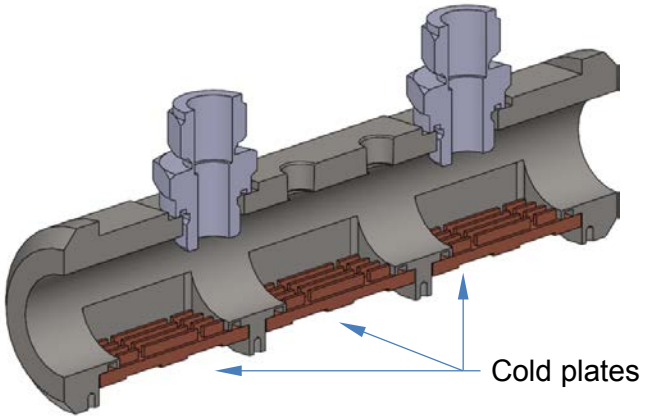

Figure 2: Cross-sectional view of the evaporator vessel.

The evaporator was designed to cool six power modules, two per cold plate. For the tests, six Watlow ceramic heaters were used in place of the power modules. The dimensions of the ceramic heaters (25 mm × 15 mm × 2.5 mm) were similar to those of the Delphi modules. Each heater generates up to about 580 W of heat (total power for six heaters: 3.5 kW). The ceramic heaters were externally attached to the evaporator using thermally conductive grease as the thermal interface material. The temperatures of the heaters were measured via thermocouples embedded within the ceramic heaters. The cold plates with attached heaters were then bolted onto the evaporator vessel. O-rings seals between the vessel and the cold plates prevented refrigerant leakage. The interchangeable cold plate design of the evaporator allows for testing of various two-phase-based cooling technologies for power electronics and other high-power density applications. The evaporator's flexible design also allows testing of different boiling/evaporation enhancement techniques (e.g., boiling enhancement coatings and finned surfaces).

The condenser consisted of a finned-tube, air-cooled heat exchanger. The fins were louvered and fabricated from 0.15 mm thick aluminum sheets (Figure 3). The total air-side surface area was calculated to be approximately 29,000 cm^2. Twenty 0.95-cm (3/8-in)-outer-diameter copper tubes were arranged in two rows (see Figure 1). Two tubes, one from each row, were connected at the top via U-bend fittings. A manifold header connected all tubes at the lower end. Two condensers were fabricated; one with plain tubes and one with rifled tubes. The rifled features, shown in Figure 3, were evaluated as a means of enhancing condensation heat transfer. Per the manufacturer, the condensation-side surface areas were 1,190 cm^2 and 1,250 cm^2 for the plain and rifled condensers, respectively. Heat from the system was rejected to air by means of a 17.8-cm (7-in) diameter automotive axial fan mounted to the condenser. The fan operates on 12 V and consumes approximately 38 W of power, calculated by voltage and current measurements. Two 2.54-cm-inner-diameter tubes connected the condenser manifold to the evaporator. The tubes were sized large enough to prevent system pressure oscillations associated with liquid entrainment by the rising vapor, within the heat load range tested.

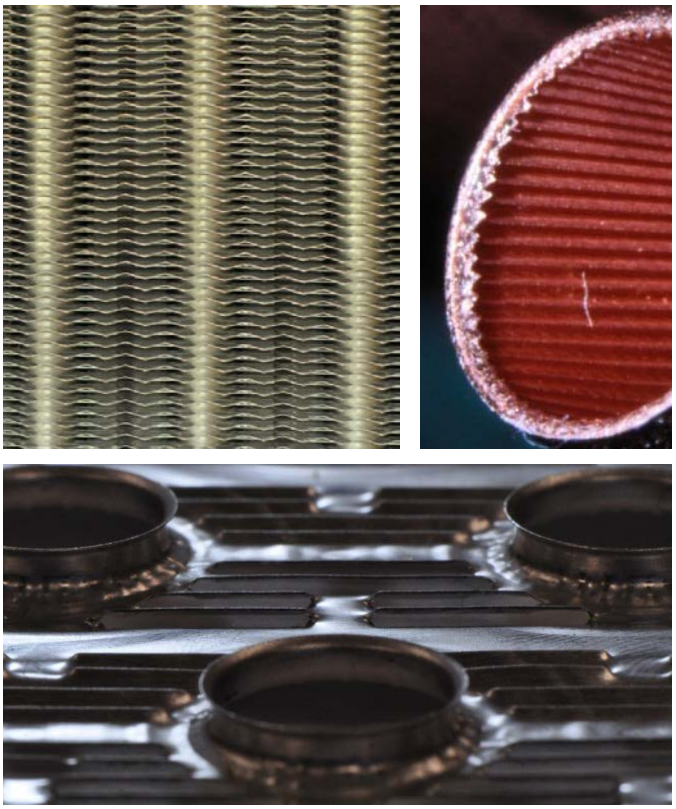

Figure 3: Images of the finned-tube condenser (top-left), rifled tube (top-right), and louvered-fin design (bottom).

Procedures were established to charge the system with refrigerant. The system was charged using a transfer tube that contained 250 cm^3 of saturated and oil-free refrigerant. This volume translated to approximately 330 grams of HFC-245fa or 280 grams of HFO-1234yf. Prior to charging the system with refrigerant, the air in the system was removed using a vacuum pump. Pressure within the system was allowed to decrease to about 2 Pa to indicate that most of the air was evacuated from the system. A valve between the transfer tube and the system was then opened, allowing 250 cm^3 of refrigerant to drain into the system. Once the refrigerant was transferred, the valve between the transfer tube and the system was closed, and the transfer tube was disconnected from the system. Measurements of the vapor temperature and pressure confirmed saturated conditions verifying that no air was present within the system.

Thermal characterization experiments were initiated after saturated conditions were verified. First, the fan was powered to pull ambient air (T_a inlet = 25°C) through the condenser. The six heaters were then powered using two Agilent direct current power supplies. Heat loads from the heaters ranged from 250 W to 3,500 W. The system was allowed to reach equilibrium conditions (about 15 minutes) at each power level before increasing the power. Measurements of the system and heater temperatures combined with heat load measurements were used to compute the evaporator and condenser thermal resistances at various power levels.

3 Uncertainty Analysis

An analysis was conducted to quantify the uncertainty in the measured experimental values according to the procedures outlined by Dieck [13]. The procedure consisted of gathering systematic and random uncertainties in all measured variables. The propagation-of-error equation was then used to estimate the uncertainties in the calculated values. The uncertainty for the thermal resistance values is estimated to be approximately ±9%. After calibration, the uncertainty in a thermocouple was conservatively estimated at ±0.1°C, while the uncertainties in the heat measurements were estimated to be ±1%. All stated uncertainties were calculated at a 95% confidence level.

4 Results and Discussion

Experiments were conducted to measure the thermal performance of the cooling system with refrigerants HFC-245fa (330 grams) and HFO-1234yf (280 grams). The unit (area-weighted) thermal resistance of the evaporator is plotted versus the heat dissipated in Figure 4. The heater-to-liquid resistance is defined per Equation 1.

$$R''_{th,\ evaporator} = \frac{(\overline{T_{htr}} - T_l)}{Total\ power} \times A_r \qquad (1)$$

where $\overline{T_{htr}}$ is the average temperature of the six ceramic heaters as measured by the thermocouples embedded within each heater, and T_l is the refrigerant liquid temperature. The *total power* is the total heat dissipated by the system, and A_r is the total surface area of the six heaters (22.5 cm^2).

Tests were performed with increasing and decreasing heat fluxes to evaluate for hysteresis effects. Results showed that using an increasing or decreasing heat rate had little effect on the thermal performance of the system.

With 250 cm^3 of HFC-245fa, the system was capable of dissipating 3.5 kW of heat under steady-state conditions without reaching dry-out (i.e., critical heat flux). The refrigerant-volume-to-heat-dissipated ratio, at maximum heat load, was 71 cm^3/kW, which is somewhat less than the 100 cm^3/kW estimate by Barnes and Tuma [5]. At 3.5 kW, the heaters are at their maximum allowable power rating, thus it was not possible to test to higher heat loads. However, results indicate the system may dissipate even greater heat loads. The 3.5 kW of heat dissipation is noteworthy because it is a conservative estimate on the inverter heat dissipation requirement for a 55-kW electric traction-drive system. With HFO-1234yf, tests were limited to lower heat loads due to HFO-1234yf's higher operating pressures. At 1.25 kW of heat dissipation, HFO-1234yf's saturated temperature reached 42°C, which corresponds to a pressure of about 1.1 MPa—the maximum operating pressure of the system. Increasing the heat dissipation with HFO-1234yf requires increasing the condensing and/or pressure capacity of the system.

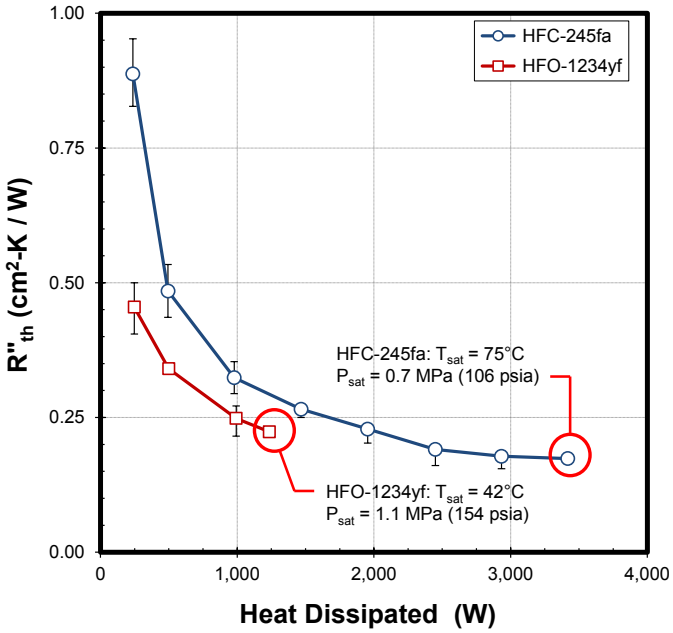

Figure 4: Averaged evaporator (heater-to-liquid) thermal resistance values versus the heat dissipated. The error bars indicate maximum and minimum values.

Because ceramic heaters attached via thermal interface material were used as a substitute for actual power modules attached via bonded interface materials (e.g., thermoplastics, solder), the thermal resistance values are not necessarily indicative of the thermal performance of the cooling system. Even so, it was still possible to draw conclusions from the thermal resistance values. Most notably, compared at the same heat loads, HFO-1234yf produced thermal resistance values that were 22% - 47% lower than those produced with HFC-245fa. HFO-1234yf's lower thermal resistance values are likely associated with a quicker onset of boiling at a lower wall superheat (at lower heat loads) and higher heat transfer rates. At a 1 kW heat dissipation, the system temperatures were approximately the same with both refrigerants (i.e., T_{sat} = 40°C in both cases). A T_{sat} of 40°C corresponds to reduced pressures of 0.07 and 0.31 for HFC-245fa and HFO-1234yf, respectively. HFO-1234yf's higher reduced pressure contributes to both its higher boiling heat transfer rates and lower boiling incipient superheat. A prior study [14], has shown that for boiling on plain copper surfaces, HFO-1234yf yields higher heat transfer rates as compared with HFC-245fa when evaluated at the same saturation temperature.

As shown in Figure 4, the heater-to-evaporator resistances for both refrigerants decrease with increasing heat dissipation. This effect is associated with an increased contribution from two-phase heat transfer (i.e., boiling/evaporation) at higher

power levels, which improves thermal performance. The system's temperature and pressure increased with increasing heat dissipation. Boiling heat transfer rates will increase with increasing pressure; thus, this effect also contributes to the observed heater-to-evaporator decreasing resistance trend.

The performance results provided in Figure 4 were obtained using an evaporator without enhanced surfaces. The use of boiling enhancement coatings such as 3M's copper microporous coating [15] within the evaporator will enable both increased heat dissipation and lower thermal resistance values. The improved performance of an advanced evaporator design employing these enhancement techniques will be discussed later.

The unit-thermal resistances for the condensers are provided in Table 1 for both refrigerants. The vapor-to-air resistance includes the condensation-side and the air-side resistances and is defined per Equation 2.

$$R"_{th,\ condenser} = \frac{(T_v - \bar{T}_a)}{Total\ power} \times A_r \qquad (2)$$

where T_v is the refrigerant vapor temperature and $\bar{T}_a$ is the average inlet air temperature as measured by two thermocouples just upstream of the condenser. *Total power* is the total heat dissipated and A_r is the frontal area (i.e., footprint) of the condenser. The stated condenser performances are for a passive condenser design cooled via an automotive axial fan. The total fan parasitic power was measured to be 38 W. An estimate of the air flow rate was calculated by imposing an energy balance on the air-side (i.e., inlet and outlet to the condenser) and the total heat dissipated. Assuming steady- state conditions and incorporating the appropriate air thermal properties, the estimated air volumetric flow rate is 0.12 m^3/s (250 ft^3 per minute).

Condensation-side enhancements from the rifled tubes were found to reduce the overall condenser thermal resistances by 18% and 25% for HFC-245fa and HFO-1234yf, respectively. The results show that the rifled structures are more effective at enhancing condensation heat transfer with HFO-1234yf. Moreover, better performance is achieved with HFO-1234yf. For the plain tube condenser, HFO-1234yf yielded thermal resistance values that were about 13% lower than those with HFC-245fa. For the rifled tube condenser, HFO-1234yf yielded thermal resistance values that were about 20% lower than those with HFC-245fa.

	R"$_{th}$ (cm^2 - K/ W)	
	Plain	Rifled
HFC-245fa	9.30	7.58
HFO-1234yf	8.12	6.06

Table 1: Condenser thermal resistance values calculated using Equation 2.

4.1 Advanced Evaporator Concept

The previously discussed work demonstrated the feasibility and performance of a passive two-phase cooling system. Knowledge gained from that work was then used to develop a more compact/lightweight evaporator with improved thermal performance. This section describes the research work related to the analysis of the advanced evaporator design and the analyses work conducted to size the system condenser.

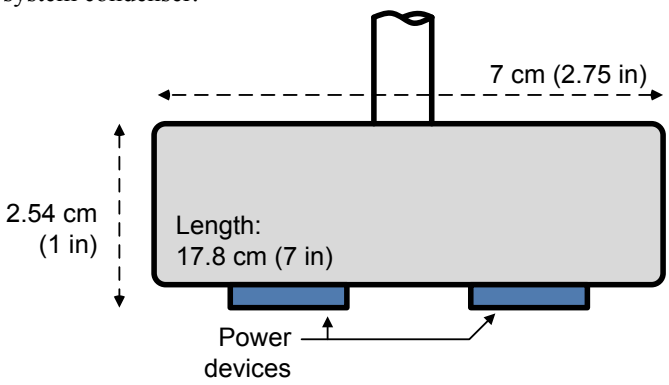

Figure 5: Simple schematic of the advanced evaporator designed to cool six power modules.

Techniques to improve the evaporator performance and reduce its size have been identified. The techniques incorporate features to reduce the evaporator thermal resistance while utilizing low-cost fabrication techniques and materials (e.g., aluminum). The concept uses an indirect cooling approach to be compatible with conventional power electronic packages (i.e., silicon on ceramic substrate).

A simple schematic of the advanced evaporator design is shown in Figure 5. To protect potentially sensitive intellectual property, certain evaporator features were omitted from the figure. The evaporator was designed to cool six Delphi discrete power switches. Although the initial tests with the proof-of-concept system were conducted using 250 cm^3 of refrigerant charge, the advanced design will utilize less refrigerant—about 180 cm^3 (HFC-245fa = 240 grams, HFO-1234yf = 200 grams). To put these quantities into perspective, a 2010 Toyota Camry requires 510 grams of refrigerant (HFC-134a) for the cabin's air-conditioning system [16]. Reducing the refrigerant quantity is an effort to reduce the system cost, weight, and size. The system design combined with the system refrigerant volume should allow for operation at various degrees of inclination. Future tests are planned to evaluate the effect of orientation on system performance.

The thermal performance of the advanced evaporator design was simulated through FEA. A computer-aided-design model of the Delphi power modules bonded to the advanced evaporator design was first generated. The computer-aided-design model incorporated all the thermal resistance interfaces within the package stack including the solder layers within the package and a thermoplastic-type bonded interface between the module and the evaporator base plate. The model was then imported into ANSYS Workbench for thermal analysis. The FEA imposed heat transfer coefficient boundary conditions to simulate boiling heat transfer from enhanced surfaces within the evaporator. In a prior studies [14, 17], the boiling heat transfer coefficients for HFC-245fa and HFO-1234yf were

experimentally measured with enhanced surfaces (3M microporous boiling enhancement coating) at various saturated temperatures. In those studies, the measured heat transfer coefficient values exceeded 100,000 W/m^2-K within a wide heat flux range. Moreover, the performance of the two refrigerants was found to be similar for boiling on microporous coated surfaces. Because uniform boiling may not occur with the evaporator surfaces, a conservative estimate on the heat transfer coefficients was imposed (50,000 W/m^2-K) for these simulations.

The unit/area-weighted thermal resistance results (junction-to-liquid) as predicted by FEA are provided in Table 2. The insulated gate bipolar transistor's area and maximum temperature (i.e., junction temperature) combined with the refrigerant temperature were used to calculate the thermal resistance values. Two evaporator designs were analyzed—aluminum-based and copper-based. The aluminum fabrication is the more practical design while the copper fabrication is more of an idealistic concept aimed at reducing the package stack resistance. For comparison, the thermal resistance (junction-to-liquid) of the 2008 Lexus Hybrid dual side and liquid (WEG)-cooled power module is also shown in Table 2. The thermal resistance value of 0.33 cm^2-K/W listed for the dual-side-cooled module was calculated using performance data from Sakai et al. [3] and the module's insulated gate bipolar transistor footprint as measured by Buress et al. [2].

	R''_{th} (cm^2 - K/ W)
Two-phase: aluminum evaporator	0.14
Two-phase: copper evaporator	0.12
2008 Lexus Hybrid, [3]	0.33

Table 2: The FEA estimated evaporator (junction-to-liquid) thermal resistances for aluminum and copper evaporators. Performance data for an automotive cooling system is provided for comparison.

The FEA predicted thermal resistance values of the aluminum (i.e., 0.14 cm^2-K/W) and copper (i.e., 0.12 cm^2-K/W) evaporator modules are about 58% and 65% lower, respectively, than that of the dual-side, WEG-cooled 2008 Lexus system. That proposed two-phase cooling configuration outperforms the dual-side-cooled (WEG coolant) package because of improved heat transfer from two-phase cooling and also because of differences in the passive stack within the packages. Future work is planned to experimentally measure the junction-to-liquid thermal resistance for the advanced evaporator design. In addition to the thermal improvements, the passive cooling approach also improves system efficiency.

An immersion cooling (two-phase) strategy may allow for even greater thermal enhancements. However, an indirect cooling approach was used in this case to allow for its use with more traditional power modules and to alleviate some reliability concerns associated with immersing electronics in a refrigerant.

4.2 Condenser Sizing Implications

An analysis was conducted to estimate condenser size based on operating conditions, a maximum allowable cooling system temperature (i.e., vapor and liquid), and the experimentally measured condenser thermal resistance values provided in Table 1. The operating conditions used for this analysis were: 3.3 kW of steady-state heat dissipation (estimated requirements for a 55 kW traction drive inverter) and 43°C inlet air temperature. The estimated condenser frontal area (i.e., frontal footprint) requirements are plotted versus the system temperature in Figure 6. In the figure, the lower system temperature of 65°C, used for this analysis, corresponds to the coolant (i.e., WEG) temperature typical of existing automotive power electronics systems. The solid line curves for both refrigerants are the sizing requirements for the finned-tube condenser per the performance data reported in Table 1. The T_j curve in Figure 6 represents the maximum junction temperature and was calculated using the thermal resistance data for an aluminum evaporator and a six power module/switch system configuration.

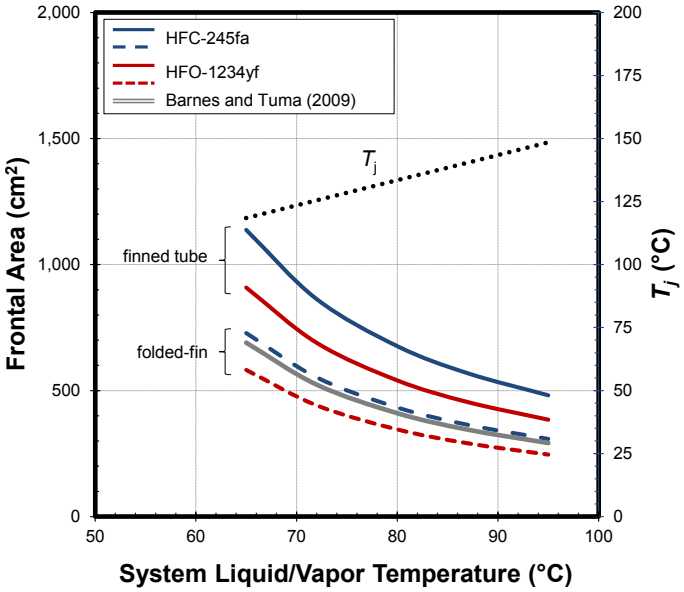

Figure 6: Condenser sizing requirements at various system temperatures. Barnes and Tuma data from [5].

Because typical automotive condensers are constructed using a brazed, folded-fin design as shown in Figure 6, a simplified analysis was conducted to estimate the sizing requirements for a folded-fin type condenser. For this analysis, the ratios of the air-side surface area to frontal surface area were measured for the finned-tube and folded-fin designs shown in Figure 7. The air-side-to-frontal-surface-area ratios were calculated to be 55.5 mm^2/mm^2 for the finned-tube and 86.7 mm^2/mm^2 for folded-fin condensers, assuming a condenser thickness of 4.5 cm for both cases. The folded-fin frontal area requirements were estimated by matching the air-side surface area for the folded-fin design to those of the finned-tube design at the various system temperatures. The folded-fin frontal area requirements were then calculated via the surface area ratio (86.7 mm^2/mm^2) and the results are shown Figure 6. This simplified analysis assumes that the air-side is the dominant thermal resistance, and air velocities are similar to those provided by the fan used

in this study. For reference, the performance of a folded-fin condenser operating in a thermosyphon configuration, as reported by Barnes and Tuma [5], is provided in Figure 6. In that study, a condenser thermal resistance of 4.6 cm^2-K/W is reported using a hydrofluoroether fluid and an air velocity and pressure drop of 2.2 m/s and 44 Pa, respectively. The estimated condenser sizing requirements, per the performance reported by [5], are similar to the results predicted for HFC-245fa.

The size requirements of the condenser can then be estimated using Figure 6 and a maximum allowable system temperature. For low-temperature applications typical of existing automotive power electronics coolant temperatures and conventional silicon devices, the use of HFO-1234yf is recommended because it provides better performance. At a system temperature of 75°C and with HFO-1234yf, the condenser frontal size requirements are estimated to be about 400 cm^2 (20 cm × 20 cm) with a maximum T_j of about 125°C. HFC-134a may also be considered in this case because it is a refrigerant currently used in automotive systems and because prior studies [17-20] have shown that its heat transfer performance (boiling and condensation) is similar, if not slightly better than, that of HFO-1234yf.

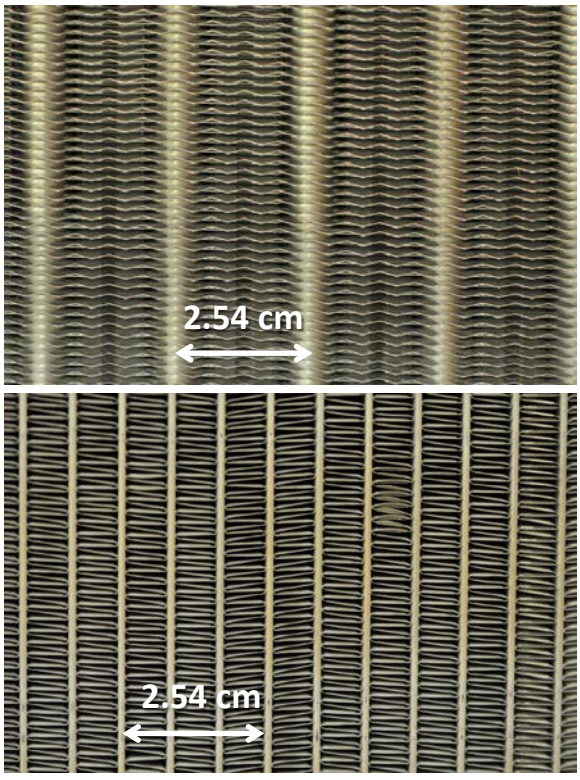

Figure 7: Images of the finned-tube condenser (top) and a brazed folded-fin condenser (bottom).

Operating at higher system temperatures has advantages because it allows for a more compact condenser. However, higher temperature operation may be dependent on the development of higher temperature auxiliary electronic devices (e.g., capacitors) that are packaged within the inverter. With this in mind, if higher system temperatures are practical, HFC-245fa is recommended due to its higher critical temperature (T_C = 154°C) and lower operating pressures. At a system temperature of 95°C and a T_j = 148°C, the condenser size requirements would decrease to about 310 cm^2 (17.6 cm × 17.6 cm).

5 Conclusions

A proof-of-concept inverter-scale passive two-phase cooling system was designed and fabricated. Experiments demonstrated that the system can dissipate at least 3.5 kW of heat with 250 cm^3 of HFC-245fa and total fan parasitic power consumption of 38 W.

The performance of the finned-tube condensers (plain and rifled) operating in the passive (thermosyphon) configuration was experimentally measured. The rifled tubes were found to decrease the thermal resistance for HFC-245fa and HFO-1234yf by 18% and 25%, respectively. Additionally, condenser thermal resistances were measured to be 13% to 20% lower with HFO-1234yf as compared with HFC-245fa.

An advanced evaporator design concept was conceived that improves thermal performance and reduces the evaporator size. The design utilized an indirect cooling configuration and thus can be used with conventional power module packages. FEA indicates the evaporator design can decrease the junction-to-liquid resistance by 58% and 65% as compared to the dual-side-cooled automotive power module.

Experimental results and analyses were used to size the system condenser based on estimated inverter operating conditions at various maximum allowable system temperatures. For low system temperature applications, HFO-1234yf is recommended, and the condenser frontal area requirements are estimated to be 400 cm^2. For higher system temperature operation, HFC-245fa is recommended due to its higher critical temperature. At a system temperature of 95°C, the condenser size can be decreased to 310 cm^2. However, higher temperature operation would likely be contingent on the development of higher temperature auxiliary power electronic devices (e.g., capacitor).

Acknowledgments

The authors would like to thank Susan Rogers and Steven Boyd, Technology Development Managers of the U.S. Department of Energy Vehicle Technologies Office, Advanced Power Electronics and Electric Motors Program, for supporting this work. They also wish to thank Charlie King (National Renewable Energy Laboratory) for helping to fabricate the experimental system and Mary Koban (DuPont) for supplying the HFO-1234yf refrigerant.

References

[1] Z. Liang, "Power Device Packaging," Oak Ridge National Laboratory, 2012 U.S. DOE Hydrogen and Fuel Cells Program and Vehicle Technologies Program Annual Merit Review, 2012.

[2] T. A. Burress, C. L. Coomer, S. L. Campbell, A. A. Wereszczak, J. P. Cunningham, L. D. Marlino, L.E. Seiber, and H.T. Lin, "Evaluation of the 2008 Lexus LS 600H Hybrid Synergy Drive System," Oak Ridge National Laboratory ORNL/TM-2008/185, 2009.

[3] Y. Sakai, H. Ishiyama, and T. Kikuchi, "Power Control Unit for High Power Hybrid System," *SAE Power*, vol. 1, 2007.
[4] C. W. Ayers, J. C. Conklin, J. S. Hsu, and K. T. Lowe, "A Unique Approach to Power Electronics and Motor Cooling in a Hybrid Electric Vehicle Environment," in *2007 Vehicle Power and Propulsion Conference, IEEE*, 2007, pp. 102-106.
[5] C. M. Barnes and P. E. Tuma, "Practical Considerations Relating to Immersion Cooling of Power Electronics in Traction Systems," *IEEE Transactions on Power Electronics,* vol. 25, pp. 2478-2485, 2010.
[6] P. E. Tuma, B. O. Fayemi, and L. J. Stang, "Condenser Design for Thermosyphons Utilizing Segregated Hydrofluoroether Working Fluids," in *Semiconductor Thermal Measurement and Management Symposium, SEMI-THERM 2007*, 2007, pp. 162-167.
[7] A. Franco and S. Filippeschi, "Closed Loop Two-Phase Thermosyphon of Small Dimensions: a Review of the Experimental Results," *Microgravity Science and Technology,* vol. 24, pp. 165-179, 2011.
[8] R. Khodabandeh, "Heat transfer in the Evaporator of an Advanced Two-Phase Thermosyphon Loop," *International Journal of Refrigeration,* vol. 28, pp. 190-202, 2005.
[9] C. Ramaswamy, Y. K. Joshi, W. Nakayama, and W. B. Johnson, "Combined effects of sub-cooling and operating pressure on the performance of a two-chamber thermosyphon," *IEEE Transactions on Components and Packaging Technologies,* vol. 23, pp. 61-69, 2000.
[10] F. Agostini, T. Gradinger, and C. de Falco, "Simulation Aided Design of a Two-Phase Thermosyphon for Power Electronics Cooling," *IECON 2011-37th Annual Conference on IEEE Industrial Electronics Society,* pp. 1560-1565, 2011.
[11] D. Khrustalev, "Loop Thermosyphons for Cooling of Electronics," in *18th IEEE Semi-Therm Symposium*, 2002, pp. 145-150.
[12] A. Pal, Y. K. Joshi, M. H. Beitelmal, C. D. Patel, and T. M. Wenger, "Design and Performance Evaluation of a Compact Thermosyphon," *IEEE Transactions on Components and Packaging Technologies,* vol. 25, pp. 601-607, 2002.
[13] R. H. Dieck, *Measurement Uncertainty: Methods and Applications*, 4 ed. Research Park Triangle Park, NC, USA: ISA, 2007.
[14] G. Moreno, J. R. Jeffers, and S. Narumanchi, "Effects of Pressure and a Microporous Coating on HFC-245fa Pool Boiling Heat Transfer " in *ASME Summer Heat Transfer Conference*, Minneapolis, MN, USA, 2013, pp. 557-567.
[15] 3M, "3M™ Microporous Metallic Boiling Enhancement Coating (BEC) L-20227," ed: 3M, 2009.
[16] AutoZone. (12/2/13). Available: http://www.autozone.com
[17] G. Moreno, S. Narumanchi, and C. King, "Pool Boiling Heat Transfer Characteristics of HFO-1234yf on Plain and Microporous-Enhanced Surfaces," *ASME Journal of Heat Transfer,* vol. 135, p. 111014, 2013.
[18] D. Del Col, D. Torresin, and A. Cavallini, "Heat transfer and pressure drop during condensation of the low GWP refrigerant R1234yf," *International Journal of Refrigeration,* vol. 33, pp. 1307-1318, 2010.
[19] J. E. Park, F. Vakili-Farahani, L. Consolini, and J. R. Thome, "Experimental study on condensation heat transfer in vertical minichannels for new refrigerant R1234ze(E) versus R134a and R236fa," *Experimental Thermal and Fluid Science,* vol. 35, pp. 442-454, 2011.
[20] K.-J. Park, D. G. Kang, and D. Jung, "Condensation heat transfer coefficients of R1234yf on plain, low fin, and Turbo-C tubes," *International Journal of Refrigeration,* vol. 34, pp. 317-321, 2011.